

# Collisionally Processed Rocks on Mars

Friedrich Hörz,<sup>1\*</sup> Mark J. Cintala,<sup>1</sup> W. C. Rochelle,<sup>2</sup> B. Kirk<sup>2</sup>

The Pathfinder landing site on Mars has boulders that may be cratered (Stimpy), split (Chimp), fragmented (Book End and Flat Top), or otherwise partly destroyed (Yogi and Frog) by collisional processes. Atmospheric-entry calculations show that centimeter-sized projectiles survive passage through the martian atmosphere and encounter the surface of Mars at velocities of a few kilometers per second. Craters less than 1 meter in diameter may contribute to the evolution of the martian surface and its soils.

The least energetic object surviving passage through a planet's atmosphere determines the smallest impact crater on the planet's solid surface. Rocks and soils from the atmosphereless moon attest to an incessant bombardment by projectiles ranging from micrometers to meters in diameter. These impactors excavate bedrock, comminute surface boulders, produce impact melts, and thoroughly garden and mix this debris to produce a global layer of fine-grained soil a few meters thick (1). Meteorite studies suggest qualitatively similar processes on atmosphereless asteroids (2). These planetary regoliths typically conceal true bedrock and, like most weathering products, they can differ mineralogically and compositionally from their source rocks. The contemporary Mars has an atmosphere of 6 mbar, some 0.016 that of Earth, thus representing an intermediate case between the moon and Earth. Past atmospheric-entry calculations differ in their estimates of the smallest projectile that would survive passage through the martian atmosphere, with associated estimates of minimum crater diameters ranging from about 2 to 3 m (3) to as large as 50 m (4). The ongoing Mars Global Surveyor Mission, however, reveals craters as small as 10 m across, essentially at the spatial-resolution limit of its imaging system (5). Here we present evidence for smaller craters, <1 m in diameter, from boulders at the Pathfinder landing site in Ares Vallis (19.33°N, 33.55°W).

Pathfinder landed on a block-strewn surface that was probably emplaced by catastrophic floods and associated debris flows, presumably about 2 billion years ago (6, 7). These boulders are characterized by a wide variety of sizes, shapes, and surface textures (Fig. 1). The prevailing interpretation is that these boulders have remained essentially unchanged since their initial deposition by en-

ergetic debris flows (8). The only subsequent major surface process appears to be wind-driven transport of fines, producing dunes, lag deposits, and fluted rock surfaces characteristic of aeolian processes (9).

Closeup views of select martian rocks are compared with analogs from experimental impacts (Fig. 2). Stimpy is a relatively rounded and fluted boulder that displays a circular depression on its top. Figure 2B illustrates an experimental hypervelocity crater, demonstrating that impacts into competent rocks have no raised rims and form shallow depressions due to pervasive spallation processes (10). Both craters abruptly terminate the rounded surfaces of their hosts, and their interiors are relatively jagged. These freshly generated surfaces on Stimpy also have an albedo that differs distinctly from the rounded, more weathered host. The circular feature on Stimpy is an impact crater about 25 cm in diameter.

The meter-sized boulder Yogi has its top terminated by a jagged fracture surface that contrasts markedly with the otherwise well-rounded host rock (Fig. 2C). We suggest that removal of Yogi's top was catastrophic, akin to the experimental analog (Fig. 2D) and sufficiently recent to preserve the jagged break. Frog (Fig. 1) appears to have suffered a similar event that dislodged a substantial portion of its top. Modestly more energetic impacts could have completely fragmented either Yogi or Frog. Collisional fragmentation experiments (11) reveal a systematic progression with increasing specific impact energy (energy per unit target mass) from craters (Stimpy) through partly destroyed hosts (Yogi, Frog), to rocks that may be split in half or, more commonly, into a small number of relatively massive fragments. We suggest that Chimp, a meter-sized, well-rounded Pathfinder boulder (Fig. 2E), may illustrate such collisional splitting, akin to the lunar analog (Fig. 2F). Additional candidates for collisionally fragmented boulders include the Book Ends, an unnamed boulder, and the Flat Top rocks. Similarly fractured rocks also occur at the Viking landing sites (12), where Big Joe is a good example.

The generation of fractures and joints,

including the fragmentation of boulders, could be due to processes other than impact. Even in the impact scenario there is no diagnostic evidence to distinguish between primary impacts at cosmic speeds, typically  $>5 \text{ km s}^{-1}$ , and collisions by secondary crater ejecta at speeds typically  $<1 \text{ km s}^{-1}$  (11). Massive boulders can be fragmented in energetic debris flows (13), but individual fragments should be separated rapidly in such a dynamic environment, beyond recognition of a common parent, contrary to the pervasive Pathfinder evidence for in situ fragmentation. We interpret the Book Ends (Fig. 1) to derive from a single slab that was fragmented after deposition, because we consider it improbable that two boulders of similar shape would by chance be deposited next to each other and in identical orientation. The unnamed boulder in Fig. 1 is also fragmented in situ, with the smaller piece barely detached from the more massive member. The Flat Top boulders, characterized by some unique jointing, also appear to have been derived from a single parent. The pervasive evidence for in situ fragmentation, which includes Yogi and Frog, argues for the disaggregation of stationary parents. Note also that the Flat Top fragments have rounded corners and wind-sculpted surfaces, whereas Yogi, Frog, and boulder 4 have jagged fractures, suggesting fragmentation events over geologically significant times.

The examples for collisional processing presented are typical for relatively modest specific impact energies sufficient to generate a few massive fragments (11). Still higher energies would completely annihilate the target, resulting in numerous small fragments. The Pathfinder site is littered with shard-like angular rocks of all sizes (Fig. 1), consistent with a description of collisional rubble, but it is not possible to associate such rocks uniquely with the collisional disruption of local



Fig. 1. Pathfinder scene with the cratered boulder Stimpy (1), partly destroyed Frog (2), and some fragmented boulders, such as Book Ends (3), an unnamed boulder (4), and the Flat Top rocks (5).

<sup>1</sup>NASA Johnson Space Center, Houston, TX 77058, USA. <sup>2</sup>Lockheed Martin, 2400 NASA Road 1, Houston, TX 77058, USA.

\*To whom correspondence should be addressed. E-mail: friedrich.p.horz@jsc.nasa.gov

REPORTS

rocks. Indeed, many could be ejecta from the 2-km Big Crater, centered about 4 km from the Pathfinder site (14).

In summarizing the photogeologic evidence, we observe a distinct dichotomy in the shapes and surface relief of Pathfinder rocks: angular, jagged fragments contrast with rounded and fluted rocks. When a single rock, such as Stimpky, Yogi, or Frog, contains both types of surfaces, the jagged surfaces are invariably superposed on the rounded shape of the rock, suggesting that fracturing occurred after rounding. Stimpky is not only rounded but also fluted (15), and the jagged surfaces are younger than the dominant ventifacts. In contrast, the Flat Tops were disaggregated early so their surfaces could become sculpted. The Pathfinder rocks reflect a variety of surface-exposure histories as postulated previously (15).

The 25-cm crater on Stimpky is smaller than predicted from the minimum projectile size that was calculated to survive atmospheric entry on Mars (3, 4). Because these earlier calculations seemed inconclusive, we employed algorithms used to predict the demise of spent spacecraft and orbital debris upon entry into the terrestrial atmosphere (16). Representative results for stony chondrites and metallic iron meteorites entering the martian atmosphere are shown in Figs. 3 and 4. All chondritic objects with a diameter of <4.3 cm vaporize at diverse altitudes. Objects initially 8 cm across reach the surface at about  $2 \text{ km s}^{-1}$ , and larger objects will have progressively higher encounter speeds. Because of the higher thermal conductivity of iron compared with chondritic material, the iron spheres initially <8.6 cm in diameter will not make it to the surface, but the smallest survivors will encounter Mars at  $>3.5 \text{ km s}^{-1}$ , faster than corresponding chondrites, because of density-related differences in effective cross section and associated drag forces.

The size of the threshold chondrite of Fig. 3A is reduced from 4.4 to 0.5 cm, and an 8-cm chondrite will be only 4.4 cm across when it impacts. Corresponding calculations for irons (Fig. 3D) reveal a minimum diameter of 3.6 cm from an object initially 8.8 cm across.

Another set of calculations varied entry velocity at a constant entry angle of  $20^\circ$  from the horizontal (Fig. 4). All objects above and to the right of a given curve of constant velocity will be destroyed during atmospheric entry, and, conversely, all objects below a specific curve will survive to the surface but at unspecified velocity and size. These calculations show that impact cratering on Mars at submeter scales can occur, although at reduced efficiency compared with the moon, because the martian projectiles will be decelerated and reduced in mass. These results are at odds with (4) but consistent with others (5, 17, 18).

We have not found centimeter-sized spall zones or melt pits, the hallmark features of

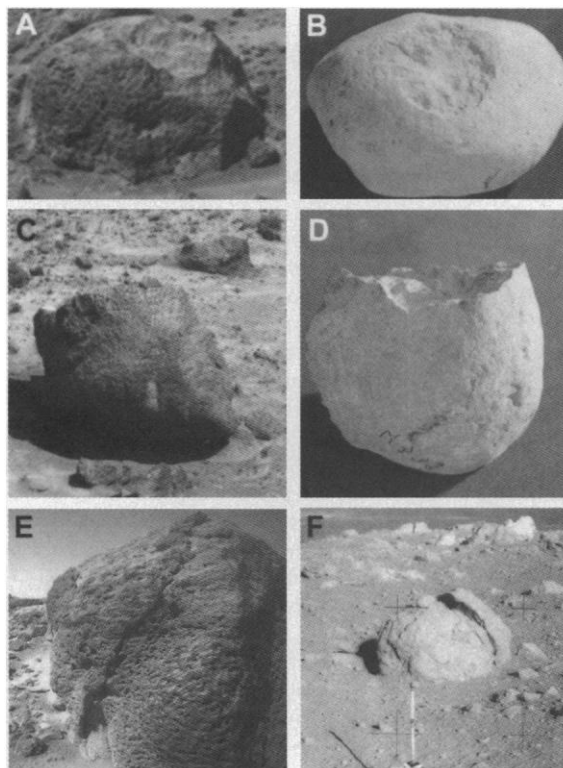


**Fig. 2.** Collisional outcomes in dense rock. (A) Spall-dominated impact crater, about 25 cm across, on Pathfinder rock Stimpky. (B) Experimental analog (10 cm in diameter) created by the impact of a 3.2-mm glass sphere at  $6.02 \text{ km s}^{-1}$  into a fluvially rounded limestone boulder. (C) Jagged, fresh break at the top of an otherwise rounded and eroded Pathfinder rock (Yogi; about 1 m tall). (D) Limestone target about 15 cm across after impact by a 6.4-mm glass sphere at  $1.7 \text{ km s}^{-1}$ —an experimental analog of Yogi. (E) Pathfinder rock Chimp with a major single fracture. (F) Lunar boulder split by an impact at the Apollo 14 site. Consult <http://mars.jpl.nasa.gov/MPF/parker/anaglyph.html> for superb stereoscopic, color images of the Pathfinder rocks.

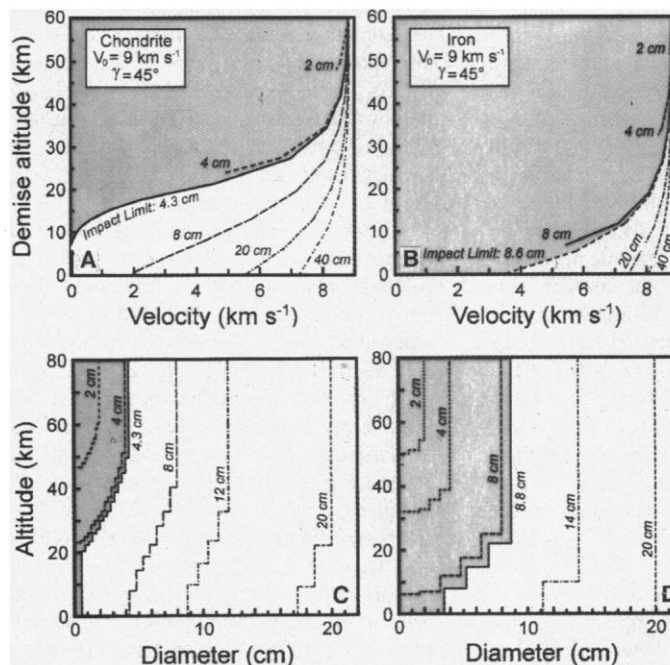


**Fig. 3.** Objects initially 2 to 100 cm in diameter that enter the atmosphere of Mars at  $9 \text{ km s}^{-1}$  and at an angle of  $45^\circ$ . Shaded area refers to sizes that do not survive atmospheric entry. (A and B) Velocity change as a function of altitude, with the velocity at zero altitude corresponding to the actual encounter speed with the surface of Mars. (C and D) Decrease in projectile diameter as a function of altitude, with zero altitude reflecting the actual impactor size at the martian surface.

impact events on lunar rocks, on any Pathfinder boulder, including those that have fluted and wind-polished surfaces that should optimize detectability of such microcraters. Cold climates could cause atmospheric  $\text{CO}_2$  to condense at the surface (17), resulting in thinner atmospheres that become increasingly more transparent to small projectiles. The absence of microcraters suggests that martian temperatures since the emplacement of the

Pathfinder rocks were probably never much colder than current conditions or that erosional environments after such cold periods were much more dynamic than the current one.

We searched in the surface images from Pathfinder and Viking landers for meter-sized craters in unconsolidated surface materials without success. This negative result is somewhat unsettling, yet we note that none of the 10-m craters observed from orbit has been re-

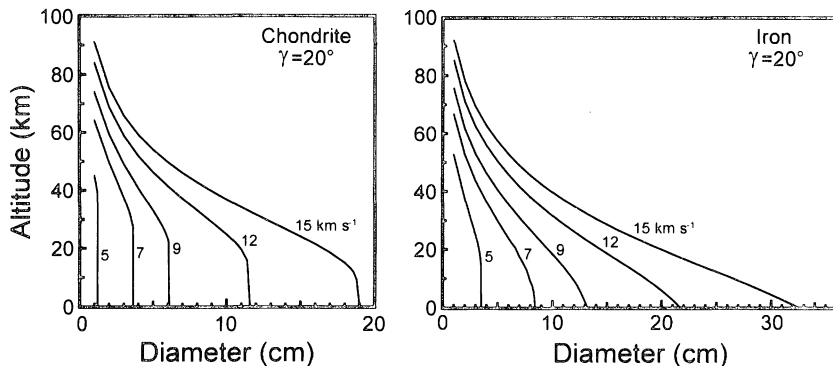


Fig. 4. Survival of chondritic and iron meteorites of various sizes that enter the martian atmosphere at a constant angle ( $20^\circ$  from the horizontal) over a range of velocities from 5 to  $15 \text{ km s}^{-1}$ .

ported in any surface images; some 100 such craters per square kilometer are recorded even on the youngest surfaces of Mars (5). Although superposition by subsequent craters and their ejecta destroyed some of these craters, the relatively old Viking and Pathfinder sites should be pervasively cratered at scales of 10 m, yet none of this cratering record is obvious in the surface images. Our search included potential secondary craters associated with Big Crater (14) that should have produced ejecta impacting at some  $100 \text{ m s}^{-1}$  at the Pathfinder site. Such velocities suffice to make craters in unconsolidated fines, yet none is recognizable. Currently we have no explanation for the apparent lack of small craters in the Pathfinder and Viking images. Compared with the highly comminuted, fine-grained lunar regoliths, the Pathfinder and Viking surfaces appear to be dominated by coarse rubble. While investigating the comminution of fragmental targets whose size distribution was dominated by fragments larger than the projectile (19), we typically produce craters that are relatively shallow and have poorly developed rims. It seems possible that martian regolith craters are similarly shallow and that they are readily modified by aeolian infill beyond recognition. Aeolian processes, however, are not energetic enough to erode the impact record in competent rocks with comparable efficiency.

Quantitative ramifications of this emerging small-scale impact environment on Mars remain to be determined and depend on the absolute impactor flux (5). Nevertheless, consistent with (5, 15), the martian surface should be more dynamic than postulated by (6, 8). Relative to the moon, the roles of craters of  $>10 \text{ m}$  will be similar on Mars, yet the effect of meter-sized events is greatly diminished, and craters smaller than a few centimeters will be absent on Mars.

References and Notes

1. H. Heiken et al., Eds. *Lunar Sourcebook* (Cambridge Univ. Press, Cambridge, 1991).  
 2. R. P. Binzel et al., Eds. *Asteroids II* (Univ. of Arizona Press, Tucson, 1989).

3. R. D. Dycus, *Publ. Astron. Soc. Pac.* **81**, 399 (1969).  
 4. D. E. Gault and R. S. Baldwin, *Eos* **51**, 343 (1970).  
 5. W. K. Hartmann, *Met. Planet. Sci.* **34**, 167 (1999).  
 6. M. P. Golombek et al., *Science* **278**, 1743 (1997).  
 7. P. H. Smith et al., *ibid.*, p. 1758.  
 8. M. P. Golombek et al., *J. Geophys. Res.* **104**, 8523 (1999).  
 9. R. Greeley et al., *ibid.*, p. 8573; N. T. Bridges et al., *ibid.*, p. 8595.  
 10. F. Hörz et al., *ibid.* **76**, 5770 (1971); D. E. Gault, *Moon* **4**, 32 (1973).

11. A. Fujiwara et al., in *Asteroids II*, R. P. Binzel et al., Eds. (Univ. of Arizona Press, Tucson, 1989), p. 240.  
 12. T. A. Mutch, *The Martian Landscape*, NASA SP 425 (1978); R. Arvidson et al., *Rev. Geophys. Space Phys.* **27**, 39 (1989).  
 13. J. W. Rice et al., *Lunar Planet. Sci.* **30**, abstr. 2063 (1999).  
 14. M. S. Stefanis and H. J. Moore, *ibid.*, abstr. 1409.  
 15. A. T. Basilevsky et al., *J. Geophys. Res.* **104**, 8617 (1999).  
 16. W. C. Rochelle et al., *Eighth Annual Thermal and Fluids Analysis Workshop*, NASA CP 3359 (1997). The calculations used the simulation and optimization of rocket trajectories (SORT) program, a trajectory code using drag coefficients of spheres in combination with the object-reentry survival analysis tool (ORSAT) subroutine, which treats aerothermal effects and ablation processes. Mars's northern-summer atmosphere [W. Hansen et al., JPL Report at COSPAR, Innsbruck, Austria (1978), p. 113] was added to SORT, along with an aeroheating subroutine for  $\text{CO}_2$  atmospheres. For additional details consult W. C. Rochelle et al., *Lunar Planet. Sci.* **30**, abstr. 1651 (1999).  
 17. A. Vasavada et al., *J. Geophys. Res.* **98**, 3469 (1993).  
 18. P. A. Bland and T. B. Smith, *Lunar Planet. Sci.* **30**, abstr. 1673 (1999).  
 19. F. Hörz and M. J. Cintala, *Met. Planet. Sci.* **32**, 179 (1997).  
 20. Discussions with R. V. Morris, A. T. Basilevsky, and M. Golombek were most helpful, as were the comments of two anonymous reviewers. We dedicate this paper to the memory of D. E. Gault, who pioneered the experimental study of planetary impacts.

1 June 1999; accepted 3 August 1999

## Defect-Mediated Condensation of a Charge Density Wave

Hanno H. Weitering,<sup>1,2</sup> Joseph M. Carpinelli,<sup>1,2</sup>  
 Anatoli V. Melechko,<sup>1,2</sup> Jiandi Zhang,<sup>3</sup> Miroslaw Bartkowiak,<sup>1,2</sup>  
 E. Ward Plummer<sup>1,2</sup>

Symmetry, dimensionality, and disorder play a pivotal role in critical phenomena. The atomic imaging capabilities of the scanning tunneling microscope were used to directly visualize the interaction between charge density oscillations and lattice defects in a two-dimensional charge density wave (CDW) system. Point defects act as nucleation centers of the CDW, which, as the temperature is lowered, results in the formation of pinned CDW domains that are separated by atomically abrupt charge boundaries. Incomplete freezing of substitutional disorder at low temperature indicates a novel CDW-mediated hopping of pinning centers.

A charge density wave (CDW) is a broken symmetry state of a metal. It incorporates a periodic modulation of the crystal's valence charge and is usually accompanied by a small periodic lattice distortion (1). In simple terms, the symmetry-breaking charge modulation (which is not necessarily commensurate with the crystal lattice) lowers the energy of the occupied electron states and raises that of the unoccupied states, opening up a band gap, so that the CDW state could become

stable below a certain critical temperature  $T_c$ . A classic example is the Peierls distortion in quasi-one-dimensional compounds such as  $\text{K}_2\text{Pt}(\text{CN})_4\text{Br}_{0.3}\cdot 3\text{H}_2\text{O}$  (known as Krogmann's salt) or transition metal bronzes such as  $\text{K}_{0.3}\text{MoO}_3$  (2). The Peierls transition is a second-order phase transition. The thermodynamic order parameter that characterizes the broken symmetry phase can be related to the magnitude of the single-particle band gap or the amplitude of the lattice distortion, which both vanish above  $T_c$ . CDW transitions in quasi-two-dimensional compounds can be first order and are not necessarily accompanied by a metal-nonmetal transition (2).

Charged impurities can alter the phase and amplitude of the condensate near the impurity

<sup>1</sup>Department of Physics and Astronomy, University of Tennessee, Knoxville, TN 37996, USA. <sup>2</sup>Solid State Division, Oak Ridge National Laboratory, Oak Ridge, TN 37831, USA. <sup>3</sup>Department of Physics, Florida International University, University Park, Miami, FL 33199, USA.

## LINKED CITATIONS

- Page 1 of 1 -



You have printed the following article:

### **Collisionally Processed Rocks on Mars**

Friedrich Horz; Mark J. Cintala; W. C. Rochelle; B. Kirk

*Science*, New Series, Vol. 285, No. 5436. (Sep. 24, 1999), pp. 2105-2107.

Stable URL:

<http://links.jstor.org/sici?sici=0036-8075%2819990924%293%3A285%3A5436%3C2105%3ACPROM%3E2.0.CO%3B2-7>

---

This article references the following linked citations:

## References and Notes

### <sup>6</sup> **Overview of the Mars Pathfinder Mission and Assessment of Landing Site Predictions**

M. P. Golombek; R. A. Cook; T. Economou; W. M. Folkner; A. F. C. Haldemann; P. H. Kallemeyn; J. M. Knudsen; R. M. Manning; H. J. Moore; T. J. Parker; R. Rieder; J. T. Schofield; P. H. Smith; R. M. Vaughan

*Science*, New Series, Vol. 278, No. 5344. (Dec. 5, 1997), pp. 1743-1748.

Stable URL:

<http://links.jstor.org/sici?sici=0036-8075%2819971205%293%3A278%3A5344%3C1743%3AOOTMPM%3E2.0.CO%3B2-4>

### <sup>7</sup> **Results from the Mars Pathfinder Camera**

P. H. Smith; J. F. Bell III; N. T. Bridges; D. T. Britt; L. Gaddis; R. Greeley; H. U. Keller; K. E. Herkenhoff; R. Jaumann; J. R. Johnson; R. L. Kirk; M. Lemmon; J. N. Maki; M. C. Malin; S. L. Murchie; J. Oberst; T. J. Parker; R. J. Reid; R. Sablotny; L. A. Soderblom; C. Stoker; R. Sullivan; N. Thomas; M. G. Tomasko; W. Ward; E. Wegryn

*Science*, New Series, Vol. 278, No. 5344. (Dec. 5, 1997), pp. 1758-1765.

Stable URL:

<http://links.jstor.org/sici?sici=0036-8075%2819971205%293%3A278%3A5344%3C1758%3ARFTMPC%3E2.0.CO%3B2-D>

**NOTE:** The reference numbering from the original has been maintained in this citation list.